Free-electron laser without inversion via transverse momentum discrimination

Dmitri E. Nikonov,[1,*] Marlan O. Scully,[2] and Gershon Kurizki[3]
[1]*Department of Physics, Texas A&M University, College Station, Texas 77843*
and Texas Laser Laboratory, Houston Advanced Research Center, Woodlands, Texas 77381
[2]*Max-Planck-Institut für Quantenoptik, Hans-Kopfermann-Strasse 1, D-85748, Garching, Germany*
[3]*Department of Chemical Physics, The Weizmann Institute of Science, Rehovot 76100, Israel*
(Received 14 February 1996; revised manuscript received 17 June 1996)

A two-stage free-electron laser with a specially designed delay of electrons in the drift region between the two wigglers allows us to obtain essentially positive gain as a function of detuning, i.e., ''lasing without inversion''(LWI). The key physical assumption is that it is *possible* to tell which electrons emit and which absorb laser energy. We here show that straightforward attempts to realize LWI operation in a free-electron laser are frequently (but not inevitably) frustrated by the difficulty of telling the difference between emitting and absorbing electrons. We propose a scheme utilizing both transverse and longitudinal components of the electron velocity to achieve cancellation of absorption. Numerical simulations verifying the validity of the scheme are presented. [S1063-651X(96)03712-9]

PACS number(s): 41.60.Cr, 52.75.Ms, 42.50.Gy, 42.50.Vk

I. INTRODUCTION

By utilizing the concept of quantum coherence and interference it has been shown that it is possible to achieve lasing without inversion (LWI) [1] in ordinary lasers [2]. These ideas have potential for application in the realm of short-wavelength laser operation. On the other hand, the question naturally arises: ''can we have LWI operation within the context of the free-electron laser (FEL)?''

In previous work [3] it has been shown that it is possible to achieve a sort of FEL operation within a LWI context in the short-wavelength (single quantum) regime. The key idea was to implement a situation in which an electron beam interacted with the laser field in two sequential regions (wigglers). In such a situation it was found that it was possible to arrange for the cancellation of absorption of radiation while at the same time retaining emission.

The notion of inversion in FEL is very different from that associated with ordinary lasers. However, the use of generalized Bloch equations for FELs [4] allows one to draw a connection between the description of a FEL and an ordinary laser, as well as to define the notion of inversion. Thus in a usual FEL net gain predominantly occurs if the majority of the electrons have the momentum above the resonant one, and loss occurs otherwise. In our FEL scheme, net gain is possible even if only a minority of the electrons are above the resonant momentum.

LWI in ordinary lasers is a result of quantum interference with no classical explanation. But is it possible that LWI operation in the FEL can be extended to the classical (many quanta of energy per electron) regime [5]? In a recent paper [6], it was argued that such a possibility exists and a tentative scheme for achieving it was proposed. In that analysis a double-wiggler configuration was again assumed, and the electrons were sorted in the drift region according to their injected energies, see Fig. 1. It was argued that it is possible to produce an asymmetric spectrum of gain, such that electrons whose injected energy is less than the resonant energy can be essentially ignored by the laser whereas electrons with injected energy greater than the resonant energy led to a net stimulated emission (see Fig. 1).

We note that there is a common feature of LWI in ordinary lasers and FELs, namely, absorption cancellation due to interference. This interference is of a quantum nature in ordinary lasers, and has a counterpart in extremely short-wavelength FELs, where a quantum description is appropriate (see [3]). Furthermore, in the classical regime, the electrons still have the phase relative to the ponderomotive potential, and can interact with a laser in such a way that radiation in one wiggler interferes destructively with radia-

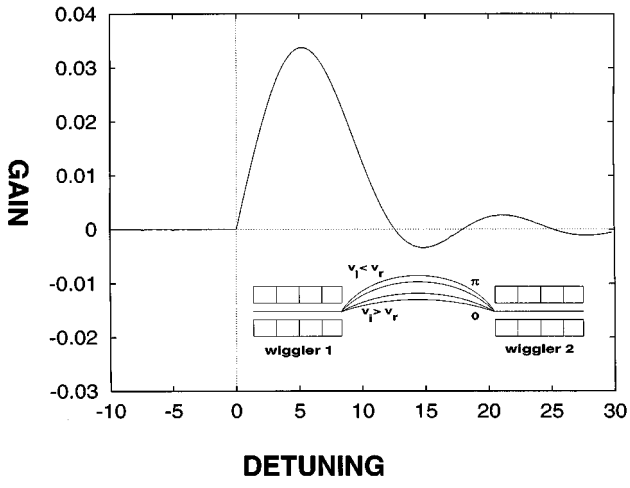

FIG. 1. The setup (lower right-hand corner) and the numerical result for the gain as a function of detuning for laser without inversion proposed in [1]; $\mathcal{N}2T=0.03$. Here and elsewhere we plot the dimensionless gain $-\langle\gamma\rangle/(\mathcal{P}8T^3)$ and detuning Ω in units of ΩT, where T is the time of flight through one wiggler, N is given by Eq. (8) and is directly related to the strength of the ponderomotive potential, and $\mathcal{P}$ governs the period of electron oscillations, see Eq. (18).

*Electronic address: nikonov@phys.tamu.edu

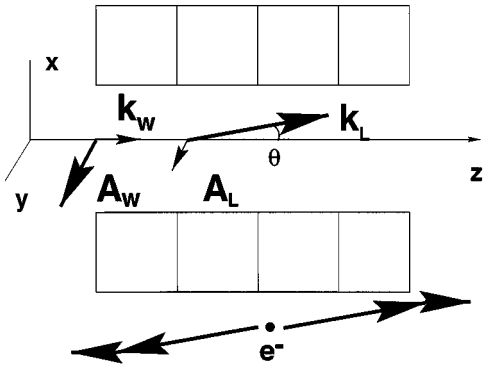

FIG. 2. Schematic of the wiggler and laser fields (top), and the momentum change in the processes of emission and absorption (bottom).

tion from another wiggler. Thus LWI is achieved via purely classical interference in the FEL.

The key physical assumption for LWI in FEL is that it is *possible* to tell which electrons emit and which absorb laser energy. We here show that straightforward attempts to realize LWI operation of the type mentioned in the preceding paragraph are frequently (but not inevitably) frustrated by the difficulty of telling the difference between emitting and absorbing electrons. Specific examples are provided in which LWI-like operation within the context of a FEL can in principle be realized.

Furthermore, we show that the correspondence between the angle of the laser field propagation and the injected longitudinal velocity can be the key for introducing a velocity-selective phase delay that cancels absorption by interference between the interaction in two consecutive wigglers. This phase-sensitive interference scheme is an example of a purely classical LWI action which does not rely on the quantum nature of matter, as it does in atomic schemes. The conclusion of the present work is that it is in principle possible to reduce the lasing threshold for electron beams with significant longitudinal velocity spread. In the following we develop these ideas in detail.

II. EQUATIONS OF MOTION AND GAIN

The classical dynamics of electrons in a free-electron laser [7] is described by the Hamiltonian [8]

$$H \equiv \gamma mc^2 = c\sqrt{(\mathbf{p}-e\mathbf{A})^2+m^2c^2}, \tag{1}$$

where m is the mass of an electron, e is the charge of an electron, c is the velocity of light, γ is referred to as the Lorentz factor, $\mathbf{p}$ is the canonical momentum, and $\mathbf{A}$ is the vector potential of the combined electromagnetic field of the wiggler, situated along the z axis (designated by a subscript W), and the laser field (designated by a subscript L), which propagates at an angle θ to the axis of the wiggler, as in Fig. 2, is

$$\mathbf{A} = 2\hat{\mathbf{y}}[A_W\cos(-\nu_W t - k_W z) + A_L\cos(-\nu_L t + k_L z\cos\theta + k_L x\sin\theta + \phi)]. \tag{2}$$

Both fields are y polarized, and ϕ is the phase of the laser field at the instant of the electron entry into the wiggler.

The Hamiltonian does not depend explicitly on y, therefore

$$\frac{dp_y}{dt} = -\frac{\partial H}{\partial y} = 0. \tag{3}$$

If the initial value of the momentum is zero, $p_y(0)=0$ [9], it remains zero at all times $p_y(t)=0$. Then the wiggling motion in this direction is described by the y component of the velocity

$$\frac{dy}{dt} = \frac{\partial H}{\partial p_y} = \frac{-eA_y}{\gamma m} \equiv v_y. \tag{4}$$

For the other coordinates

$$\frac{dz}{dt} = \frac{\partial H}{\partial p_z} = \frac{p_z}{\gamma m} \equiv v_z, \quad \frac{dx}{dt} = \frac{\partial H}{\partial p_x} = \frac{p_x}{\gamma m} \equiv v_x. \tag{5}$$

In the equations for the derivatives of the momenta there are terms of interaction with the fields having various dependences on the time and the coordinates. Of those, following a standard procedure [10], we drop (an analog of a rotating-wave approximation) the terms that are rapidly oscillating in the frame of reference of an electron moving with the injected velocity $v_i < c$ but close to c. The remaining (''near-resonant'') terms oscillate slowly in this frame of reference. In this way we obtain the equations of motion for the energy and momenta (see the Appendix),

$$\frac{d\gamma}{dt} = \mathcal{N}\sin(-\Delta\nu t + q_z z + q_x x + \phi), \tag{6}$$

$$\frac{mc^2}{\Delta\nu}\frac{d\gamma}{dt} = \frac{1}{q_z}\frac{dp_z}{dt} = \frac{1}{q_x}\frac{dp_x}{dt}, \tag{7}$$

where

$$\mathcal{N} = \frac{e^2 2A_W A_L \Delta\nu}{m^2c^2\gamma}. \tag{8}$$

The argument of the sin function in Eq. (6) is the phase relative to combined action of the wiggler and laser fields (''ponderomotive potential''),

$$\psi = -\Delta\nu t + q_z z + q_x x + \phi. \tag{9}$$

Equation (7) expresses the relation between the momentum ($q_x = k_L\sin\theta$, $q_z = k_L\cos\theta + k_W$) and energy ($\Delta\nu = \nu_L - \nu_W$) transfer in each act of a photon emission or absorption (see Fig. 2) [11].

Gain in the case of electrons injected with a certain initial energy (''cold beam regime'') is proportional to the flux of electrons and the change of energy of all the electrons averaged (which is designated by $\langle\ \rangle$) over the uncontrollable phase at the injection $G \propto -\langle\Delta\gamma\rangle$. The dynamical equations simplify in the case when electron energy γ does not differ very much from the injected energy γ_i or a certain resonant energy γ_r and the longitudinal coordinate and velocity differ

by a small amount from a uniform motion with the injected velocity; $z=v_i t+\delta z$ and $v_z=v_i+\delta v_z$. The equations of motion become

$$\frac{d\gamma}{dt}=\mathcal{N}\sin(\Omega t+q_z\delta z+q_x x+\phi). \tag{10}$$

Here

$$\Omega=q_z v_{zi}-\Delta\nu\equiv q_z(v_{zi}-v_r) \tag{11}$$

is the detuning of an electron from the resonance with the ponderomotive potential, and

$$v_r=q_z/\Delta\nu \tag{12}$$

is its velocity corresponding to the resonant energy γ_r. The equations for the velocity components (see the derivation in the Appendix) are

$$\frac{dv_z}{dt}=\frac{q_z c^2}{\Delta\nu\gamma_r^3}\frac{d\gamma}{dt}, \tag{13}$$

$$\frac{dv_x}{dt}=\frac{q_x c^2}{\Delta\nu\gamma_r}\frac{d\gamma}{dt}. \tag{14}$$

The equations demonstrate that there is a one-to-one correspondence between the infinitesimal change of each component of the velocity and the change of energy. These equations, though describing a two-dimensional motion, result in the pendulum equation with the phase ψ,

$$\ddot{\psi}=\frac{\mathcal{P}}{\mathcal{N}}\sin\psi, \tag{15}$$

$$\psi(0)=\phi, \tag{16}$$

$$\dot{\psi}(0)=\Omega, \tag{17}$$

$$\mathcal{P}=\frac{\mathcal{N}^2c^2}{\gamma_r^3\Delta\nu}(\gamma_r^2q_x^2+q_z^2). \tag{18}$$

It is seen from Eq. (15) that the motion in the wigglers is effectively one dimensional, i.e., similar to that with $q_x=0$. However, this is not true for the drift region, where the two-dimensional dynamics of the electrons is different from the one-dimensional case.

III. PERTURBATIVE DESCRIPTION OF MOTION

An analytical solution to the above equations can be obtained in a perturbation series in the laser amplitude (in the small parameter $\mathcal{N}2T$, see further), following the method of [10]. The indices I and II refer to the first and the second wiggler, respectively. In the zeroth order of perturbation, the coordinates δz and x vanish, which yields

$$\frac{d\gamma_{\mathrm{I}}^{(0)}}{dt}=\mathcal{N}\sin(\Omega t+\phi). \tag{19}$$

When averaged over injection phases, the net change of the energy (and consequently gain) is zero in this order.

In the next order in the lasing field, the coordinates are from (14),

$$\delta z^{(1)}(t)=\frac{q_z c^2}{\Delta\nu\gamma_r^3}\int_0^t\Delta\gamma_{\mathrm{I}}^{(0)}(t')dt', \tag{20}$$

$$x^{(1)}(t)=\frac{q_x c^2}{\Delta\nu\gamma_r}\int_0^t\Delta\gamma_{\mathrm{I}}^{(0)}(t')dt'. \tag{21}$$

Expansion of (10) around the solution (19) with the above coordinates gives

$$\frac{d\gamma_{\mathrm{I}}^{(1)}}{dt}=\mathcal{P}\cos(\Omega t+\phi)\mathcal{N}^{-1}\int_0^t\Delta\gamma^{(0)}(t')dt'. \tag{22}$$

When integrated over time and averaged over the injection phases, the change of energy, and consequently gain, is nonzero in this order of perturbation.

In order to focus on the effects of interference of radiation processes, we will consider interaction in two identical wigglers of length L_W with a drift region between them, in accord with the setup in our previous work [6]. The time it takes an electron to traverse a wiggler is $T\approx L_W/v_r$. The effect of the drift region is an addition of phase delay $\Delta\psi$ in the second wiggler relative to the first one, which, from examining (9), is seen to be

$$\Delta\psi=\left(s_L-\frac{s_e c}{v}+x_{\mathrm{II}}\sin\tilde{\theta}-x_{\mathrm{I}}\sin\theta\right), \tag{23}$$

where s_e and s_L are the paths of an electron and of the light wave in the drift region, respectively, $\tilde{\theta}$ is the angle of propagation of the laser in the second wiggler, x_{I} and x_{II} are the transverse coordinates at the exit from the first wiggler and at the entrance to the second wiggler, and v is the absolute value of the electron velocity which is not changed in a purely magnetic field of the drift region. The optical klystron [12] is a specific case of this phase delay with $x_{\mathrm{I}}=x_{\mathrm{II}}=0$ and $s_e=s_L$, but it is not considered here.

Then the change of energy in the second wiggler is given by

$$\frac{d\gamma_{\mathrm{II}}^{(0)}}{dt}=\mathcal{N}\sin(\Omega t+\phi+\Delta\psi), \tag{24}$$

$$\frac{d\gamma_{\mathrm{II}}^{(1)}}{dt}=\mathcal{P}\cos(\Omega t+\phi+\Delta\psi)\mathcal{N}^{-1}\int\Delta\gamma^{(0)}dt'. \tag{25}$$

Application of Eqs. (22) and (25) yields the phase averaged energy change in the whole laser,

$$\begin{aligned}\langle\Delta\gamma^{(1)}\rangle=\frac{\mathcal{P}}{2\Omega^3}[&2\Omega T\sin\Omega T+4\cos\Omega T-4+2\Omega T\sin\\&\times(2\Omega T+\Delta\psi)-2\Omega T\sin(\Omega T+\Delta\psi)\\&+2\cos\Delta\psi+2\cos(2\Omega T+\Delta\psi)\\&-4\cos(\Omega T+\Delta\psi)].\end{aligned} \tag{26}$$

For the case of a usual FEL ($\Delta\psi=0$) this gives the well-known expression

$$\langle \Delta\gamma \rangle = (2T)^3 \mathcal{P} \frac{1}{8} \frac{d}{d\alpha} (\mathrm{sinc}^2 \alpha)|_{\alpha=\Omega T}, \tag{27}$$

where $\mathrm{sinc}\alpha \equiv \sin\alpha/\alpha$.

For the case of the laser without inversion proposed in our previous work [6] the phase delay was chosen to be

$$\Delta\psi = \begin{cases} 0 - q_z(v_{zi} - v_r)T \equiv 0 - \Omega T, & v_{zi} > v_r \\ \pi - q_z(v_{zi} - v_r)T \equiv \pi - \Omega T, & v_{zi} < v_r . \end{cases} \tag{28}$$

In this case

$$\langle \Delta\gamma \rangle = \Theta(\Omega)(2T)^3 \mathcal{P} \frac{1}{16} \frac{d}{d\alpha} (\mathrm{sinc}^2 \alpha)|_{\alpha=\Omega T/2}, \tag{29}$$

and we see that absorption is completely canceled for the negative detunings [13].

The maximum gain for LWI is lower than for a usual laser, but its advantage is manifested under conditions of a broad electron distribution $g(v - \overline{v})$ over injected energies (''hot beam regime''). Gain in this regime is obtained via the expression for the gain of a monoenergetic electron beam,

$$G_{\mathrm{hot}}(\overline{v}) = \int G(\Omega(v'))g(v' - \overline{v})dv'. \tag{30}$$

Then the integral of the gain curve is important,

$$I_g = -\int \langle \Delta\gamma \rangle d(2\Omega T). \tag{31}$$

If it is nonzero, the gain for the broad distribution is proportional to the inverse width of the distribution. If the integral I_g is zero, the gain is much less: proportional to the square of the inverse width (see [6]). For a usual FEL the integral (31) *over only positive detunings* is

$$I_g = (2T)^3 \mathcal{P} \frac{1}{4}, \tag{32}$$

and the integral has exactly the opposite value over the negative detunings, so that the overall integral is *zero*. For the LWI case the integral over the negative detunings is zero, and the integral over positive detunings still has the value (32), i.e., 1/4, disregarding the constant factors, so that the overall integral is positive.

We performed numerical simulation of the electron dynamics using Eqs. (10)–(14) without the small field approximation. The unitless gain for the LWI scheme is shown in Fig. 1. It is in an excellent agreement (the difference cannot be resolved in this plot) with the analytical result (29) even for moderate laser amplitudes.

IV. SINGULARITY IN ONE-DIMENSIONAL MOTION

However, there are subtleties associated with the straightforward application of these ideas to the FEL. The root of the difficulty is that the equipment producing the phase delay (e.g., the magnetic field in the drift region) will have as an initial condition the velocities v_z of electrons as they exit from the first wiggler. This is, of course, different from the initial velocity v_{zi} with which they enter the first wiggler.

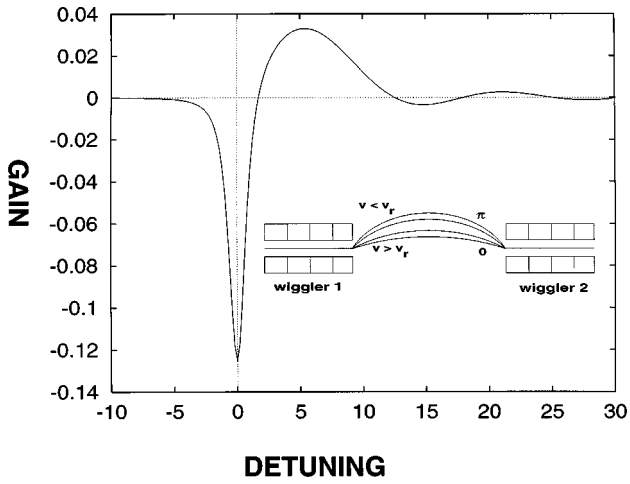

FIG. 3. Implementation of LWI using the exit velocities of electrons from the first wiggler (inset) as per phase delay given in Eq. (33). The numerical result for the gain; $\mathcal{N}2T = 0.03$, the step function is smoothed to the slope of 1 in units of ΩT.

Therefore instead of (28), the phase delay will be given by

$$\Delta\psi = \begin{cases} 0 - q_z(v_z - v_r)T, & v_z > v_r \\ \pi - q_z(v_z - v_r)T, & v_z < v_r . \end{cases} \tag{33}$$

Since the change of the velocity is small, it is reasonable to think that the phase delays (28) and (33) would be essentially the same. However, this is not the case and the gain turns out to be significantly altered. The result of numerical solution using Eqs. (10)–(14) for the case of the delay (33) is shown in Fig. 3. The integral of this function is found to be zero.

The reason for the sharp spike close to the resonance is the peculiar behavior of electrons in the vicinity of the velocity v_r where the step of the phase delay occurs. To this end, we note that electrons with initial velocity less than (but near to) v_r can end up with velocity greater than v_r and be indistinguishable from the electrons injected with velocity greater than v_r, see Fig. 4; and vice versa for electrons with velocity initially greater than v_r.

Even for the case of a very weak laser field (which therefore implies a small velocity change) the role of the electrons in the vicinity of v_r is crucial. In the vicinity of v_r the above described perturbation procedure has a singularity. The change of energy averaged over the injection phases does not

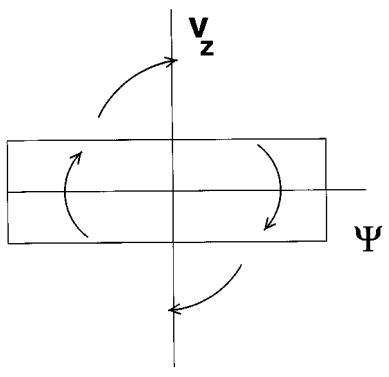

FIG. 4. Diagram showing electron energy and phase change close to the step separating phase-delay domains.

vanish in the zeroth order of perturbation. However, outside this vicinity, such that none of the electrons will cross v_r, the gain is the same as given in the preceding section.

To express this quantitatively we recall the expression for the change of energy in the first wiggler and the second wiggler,

$$\Delta\gamma_{\mathrm{I}}=\mathcal{N}T\sin(\tilde{\phi})\mathrm{sinc}(\Omega T/2), \tag{34}$$

$$\Delta\gamma_{\mathrm{II}}=\mathcal{N}T\sin(\tilde{\phi}+\Omega T+\Delta\psi)\mathrm{sinc}(\Omega T/2), \tag{35}$$

where $\tilde{\phi}=\phi+\Omega T/2$. Depending on their injected energies and phases, the electron will acquire different energy changes. Let the electrons with phases $\sin(\tilde{\phi})=\delta$ move from a specific injected energy to exactly the energy where the step occurs (γ_r in our case). As before, the energy change in the first wiggler averaged over the injection phases is zero in this order of perturbation. In the second wiggler, the energy change averaged over the intervals of electron phases $\sin\tilde{\phi}>\delta$ and $<\delta$,

$$\langle\Delta\gamma_{\mathrm{II}}\rangle=\pm\mathcal{N}T\cos(\Omega T+\Delta\psi)\frac{1}{\pi}\sqrt{1-\delta^2}\,\mathrm{sinc}(\Omega T/2), \tag{36}$$

where the plus corresponds to the first interval, and the minus corresponds to the second interval. One of these intervals corresponds to the electrons that did, and the other interval to the electrons that did not cross the energy where the step occurs.

Averaging over the phases at a specific energy, in general, gives a narrow peak (dip) close to the step with the half-width

$$\gamma_{\mathrm{width}}=\mathcal{N}T|\mathrm{sinc}(\Omega T/2)|. \tag{37}$$

Then the integral of the energy change over one of the two halves of the peak is

$$I_{g,\mathrm{peak}}=\mp(2T)^3\mathcal{P}\mathrm{sinc}^2(\Omega T/2)\cos(\Omega T+\Delta\psi)\frac{1}{8}, \tag{38}$$

where now the minus corresponds to the electrons with the injected energy above the step and the plus to those with the energy below the step. These analytical results coincide with the numerical modeling. For the phase delay (33) the area of the peak (actually the dip) in a small vicinity of zero detuning is opposite to the expression (32). Combined with the zero integral over negative detunings and still the same ''1/4'' integral over the positive detunings as given by (32), the overall integral vanishes.

V. TWO-DIMENSIONAL MOTION

In the preceding section we have seen that the goal of absorption cancellation is not achieved in the simple version of the scheme due to the peculiar behavior of electrons near the phase-delay step. The phase delay consists of two parts: the smooth velocity-dependent part $q_z(v-v_r)$ aimed at compensating for the bunching in the first wiggler and the step-like velocity-dependent part changing the phase delay from 0 to π. We consider the step to be sharp, but the numerical calculations show that the effect is still present if its width is comparable with the homogeneous width. This step existed as a function of the velocity at the exit from the first wiggler. Due to even very small changes in energy, the electrons were experiencing a phase delay very much different from the optimum one. Hence we come to the conclusion that absorption cancellation can only be realized if the steplike part is a function of the injected velocity. The smooth part can still be the function of the exit velocity from the first wiggler without affecting the gain significantly. Thus we aim at implementing the following delay function:

$$\Delta\psi=\begin{cases}0-q_z(v_z-v_r)T, & v_{zi}>v_r\\ \pi-q_z(v_z-v_r)T, & v_{zi}<v_r.\end{cases} \tag{39}$$

To implement such a delay function, a somewhat more sophisticated scheme is envisioned. First let us examine more closely the changes in the velocities in the first wiggler. From Eqs. (13) and (14) we find

$$\frac{dv_x}{dv_z}=\frac{q_x\gamma_r^2}{q_z}\approx\gamma_r^2\sin\theta, \tag{40}$$

the last equality made in the approximation of a small angle θ and $k_L\gg k_W$. Even though $\sin\theta\sim0.01$, the proportionality coefficient may be large, since $\gamma\sim100$.

The changes of the velocities are depicted in Fig. 5(a). Here the initial positions of electrons with the same initial velocity are shown as white circles. The final states of electrons are shown with the black circles. The electrons with the same initial velocity now lie along a line with the slope determined by (40). Electrons initially at resonance move symmetrically in both directions along the line. Electrons initially above resonance move preferably to lower energies rather than to higher energies, while the electrons initially below resonance move preferably to higher energies. This illustrates the gain mechanism discussed in Sec. III. Figure 5 allows us to see the same process in a different picture, i.e., to see how the initial phase determines the change of the longitudinal velocity. The amount of velocity change is determined by the detuning and the injection phase, but the changes of the velocity components are proportional. Integrating (40), we see

$$v_x=\gamma_r^2\sin\theta(v_z-v_{zi}), \tag{41}$$

hence the transverse velocity bears the memory of the initial velocity. It becomes, in fact, possible to distinguish by the transverse component the electrons that experienced net emission from those that experienced net absorption.

In the previous sections, even though the motion might have been two dimensional (in x and z directions), this fact was not used for interference. In the present scheme we use *both* the longitudinal and the transverse components of the velocity at the exit from the first wiggler to determine the phase delay (see Fig. 6). As seen from Fig. 5, the electrons with initial velocity below resonance end up in the upper half plane bordered by the line

$$v_x=\gamma_r^2\sin\theta(v_z-v_r). \tag{42}$$

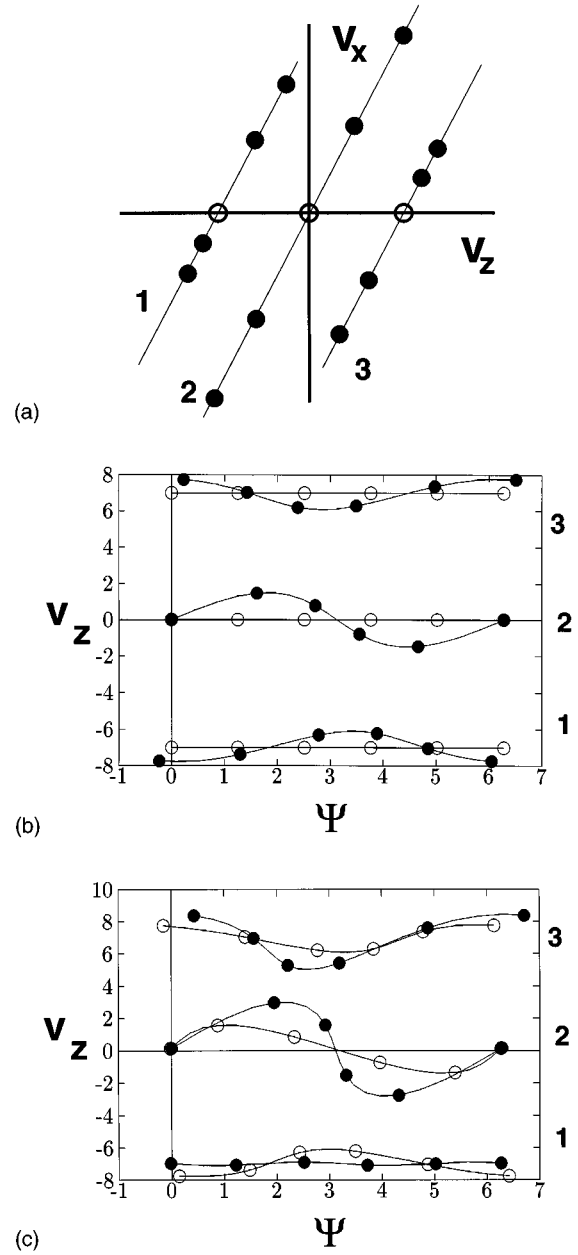

FIG. 5. In all plots open circles are initial states of electrons, solid circles are final states of electrons with different initial phases. Lines connect electrons with the same initial velocity and different phases. Curve 1 designates the electrons injected below resonance, curve 2 electrons injected at resonance, and curve 3 electrons injected above resonance. Longitudinal velocity has origin at resonance. Plots (a) and (b) describe the effect of the first wiggler on electrons. (a) Schematic of changes of longitudinal and transverse velocity components in the first wiggler. The axes have different scales. Electrons with the same initial energy are positioned along straight lines as per Eq. (41). (b) The corresponding motion in phase-velocity coordinates. The open circles correspond to the initial state, and the solid circles correspond to the final state. The area between the final and the initial curves is positive for 1 (loss), zero for 2, negative for 3 (gain). (c) Same as (b), but open circles (solid circles) correspond to entrance to (exit from) second wiggler. Key point is that curve 1 shows electrons have neither gained nor lost energy after traversing both wigglers with appropriate phase delay as given by Eq. (39).

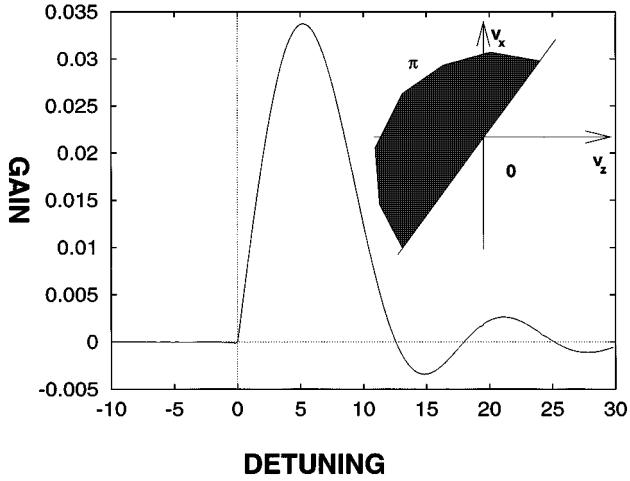

FIG. 6. The implementation of LWI using both longitudinal and transverse components of the velocity as per Eq. (39) (upper right-hand corner); numerical result for the gain; $\mathcal{N}2T=0.03$.

The electrons with initial velocity higher than the resonant one are now below this line. Then the step needs to be arranged along this line, as it is shown in Fig. 6.

Practically this modification is achieved by setting the laser cavity at some angle with the wiggler as in Fig. 2. The electrons will enter the drift region at different angles depending on their transverse velocity. By their deflection in the magnetic field, they will receive a phase delay corresponding to the smooth part of the delay function [6]. In addition, the electrons from only one side of (42) will be sent to a region of magnetic field with sharp boundaries, where they travel an additional path corresponding to the phase π. This implements the step part of the phase delay [14].

The analytical expression for the gain is very complicated in this case. For numerical simulation of this situation we have to solve Eqs. (10)–(14) taking into the account the transverse motion, and to introduce the phase shift in the drift region depending on both components of the velocity. The result for the case of phase delay (39), Fig. 6, shows that the original LWI result is recovered.

ACKNOWLEDGMENTS

D.E.N. and M.O.S. wish to thank A. M. Sessler, M. Xie, and K. J. Kim for stimulated and helpful discussions; and gratefully acknowledge support from the Office of Naval Research, the Welch Foundation, and the Texas Advanced Research and Technology Program.

APPENDIX

Because the present two-dimensional problem is somewhat different from the usual one-dimensional analysis, we provide here some intermediate steps in the derivation of formulas used in the paper.

Provided that $p_y(t)=0$, the Hamiltonian (1) becomes

$$H\equiv\gamma mc^2=c\sqrt{p_z^2+p_x^2+e^2A_y^2+m^2c^2}. \tag{A1}$$

Then

$$\frac{mc^2 d\gamma}{dt} = \frac{\partial H}{\partial t} = \frac{e^2}{\gamma m}\frac{\partial}{\partial t}\left(\frac{A_y^2}{2}\right), \tag{A2}$$

$$\frac{dp_z}{dt} = -\frac{\partial H}{\partial z} = -\frac{e^2}{\gamma m}\frac{\partial}{\partial z}\left(\frac{A_y^2}{2}\right), \tag{A3}$$

$$\frac{dp_x}{dt} = -\frac{\partial H}{\partial x} = -\frac{e^2}{\gamma m}\frac{\partial}{\partial x}\left(\frac{A_y^2}{2}\right). \tag{A4}$$

The square of the vector potential (2) is given by

$$\frac{A_y^2}{2} = 2A_W^2\cos^2(\nu_W t + k_W z) + 2A_L^2\cos^2(\nu_L t - k_L\cos\theta z - k_L\sin\theta x - \phi) + 2A_W A_L[-\cos(\nu_W t + k_W z + \nu_L t - k_L z\cos\theta - k_L x\sin\theta - \phi) + \cos(-\nu_W t - k_W z + \nu_L t - k_L z\cos\theta - k_L x\sin\theta - \phi)]. \tag{A5}$$

Only the last term can be slowly oscillating in the electron frame of reference, the other three are thrown away in the rotating-wave approximation. The phase of the remaining term is

$$\psi = -(\nu_L - \nu_W)t + (k_W + k_L\cos\theta)z + k_L x\sin\theta + \phi. \tag{A6}$$

Substitution of (A5) into (A4) yields the equations of motion

$$\frac{dp_z}{dt} = \frac{e^2}{\gamma m}2A_W A_L(k_L\cos\theta + k_W)\sin\psi, \tag{A7}$$

$$\frac{dp_x}{dt} = \frac{e^2}{\gamma m}2A_W A_L k_L\sin\theta\sin\psi, \tag{A8}$$

$$\frac{d\gamma}{dt} = \frac{e^2}{\gamma m^2 c^2}2A_W A_L(\nu_L - \nu_W)\sin\psi, \tag{A9}$$

which are equivalent to Eqs. (6) and (7).

To obtain these equations in terms of the velocity, we need the kinematic relations (5),

$$p_z = \gamma m v_z, \tag{A10}$$

$$p_x = \gamma m v_x. \tag{A11}$$

Upon substitution to the Hamiltonian (A1) one obtains

$$c^2 = v_z^2 + v_x^2 + c^2(1 + a_y^2)\frac{1}{\gamma^2}, \tag{A12}$$

where the dimensionless vector potential is

$$a_y = \frac{eA_y}{mc}. \tag{A13}$$

Further for simplicity we consider it much less than unity; the generalization for large vector potentials is trivial.

Next we differentiate the above kinematic relations. Later we take them at the point of unperturbed motion of the electron at resonance, when $v_x = 0 = p_x$, and the longitudinal variables $v_z = v_r$, $p_z = p_r$, $\gamma = \gamma_r$. Then from (A12)

$$\gamma^3 v_z dv_z = c^2 d\gamma. \tag{A14}$$

Differentiation of (A1) yields

$$mc^2 d\gamma = v_z dp_z, \tag{A15}$$

and from these

$$dp_z = \gamma^3 m dv_z. \tag{A16}$$

Differentiation of (A11) gives

$$dp_x = \gamma m dv_x. \tag{A17}$$

From the above two equations we conclude that the transverse mass of a relativistic electron is $m\gamma$ and the longitudinal mass is $m\gamma^3$.

Upon substituting the explicit expression for the resonant velocity

$$v_z = v_r \equiv \frac{\Delta\nu}{q_z}, \tag{A18}$$

Eq. (A15) coincides with the dynamic equation (7); Eq. (A14) results in Eq. (13):

$$\frac{dv_z}{dt} = \frac{q_z c^2}{\Delta\nu\gamma_r^3}\frac{d\gamma}{dt}$$

and, together with Eq. (7), Eq. (A17) yields Eq. (14):

$$\frac{dv_x}{dt} = \frac{q_x c^2}{\Delta\nu\gamma_r}\frac{d\gamma}{dt}.$$

[1] O. Kocharovskaya and Y. Khanin, Pis'ma Zh. Éksp. Teor. Fiz. **48**, 581 (1988) [JETP Lett. **48**, 630 (1988)]; S. E. Harris, Phys. Rev. Lett. **62**, 1033 (1989); M. O. Scully, S. Y. Zhu, and A. Gavrielides, *ibid.* **62**, 2813 (1989).

[2] A. S. Zibrov *et al.*, Phys. Rev. Lett. **75**, 1499 (1995); G. G. Padmabandu *et al.*, *ibid.* **76**, 2053, (1996).

[3] G. Kurizki, M. O. Scully, and C. Keitel, Phys. Rev. Lett. **70**, 1433 (1993); D.E. Nikonov, B. Sherman, G. Kurizki, and M.O. Scully, Opt. Commun. **123**, 363 (1996).

[4] H. Al Abawi, F. A. Hopf, and P. Meystre, Phys. Rev. A **16**, 666 (1977).

[5] We note that the difficulties associated with an antisymmetric gain-absorption curve are circumvented in the high-gain regime of a FEL operation, see R. Bonifacio, C. Pellegrini, and L. Narducci, Opt. Commun. **50**, 373 (1984); R. Bonifacio *et al.*, Riv. Nuovo Cimento **13**, 1 (1990). D. E. Nikonov, Yu. V. Rostovtsev, and M. O. Scully plan to consider the high-gain regime for the FEL without inversion in future work.

[6] B. Sherman, G. Kurizki, D. E. Nikonov, and M. O. Scully, Phys. Rev. Lett. **75**, 4602 (1995).

[7] C. A. Brau, *Free-Electron Lasers* (Academic, Boston, 1990); G. Dattoli, A. Renieri, and A. Torre, *Lectures on the Free Electron Laser Theory and Related Topics* (World Scientific, London, 1993).

[8] We consider low enough currents and correspondingly low enough densities in the electron beam so it is possible to neglect the Coulomb interaction between the electrons, and thus to consider the motion of electrons separately.

[9] For the purposes of the present discussion we disregard the distribution in the initial transverse velocities and consider only the distribution in longitudinal velocities. This treatment is valid until the initial transverse velocities are less than its variation (14) due to the interaction with the wiggler. This gives a limitation for the normalized emittance of $\epsilon_n \leqslant 0.1$ mm mrad for a beam width of 10^{-4} m and characteristic values of parameters assumed in the paper. This value is an order of magnitude beyond that of the present technology. However, one should expect qualitatively similar phenomena at higher emittance values.

[10] A. Yariv, *Quantum Electronics* (John Wiley, New York, 1989), Chap. 13.

[11] We note that the momentum-energy relation (7) and all the following results apply to other cases of polarizations of the fields as well.

[12] N. A. Vinokurov and A. N. Skrinsky, Institute of Nuclear Physics (Novosibirsk) Report No. INP77-59, 1977 (unpublished); N. A. Vinokurov, in Proceedings of the 10th International Conference on High Energy Particle Accelerators, Serpukhov, 1977 [Institute of Nuclear Physics, Siberian Branch, USSR Academy of Science Report No. IYAF77-59, 1977 (unpublished)].

[13] An interesting precursor to the present considerations is to be found in the ''echo effects in the FEL'' studies, see P. Meystre *et al.*, Opt. Commun. **29**, 87 (1979).

[14] Yet it is important to ask what price is to be paid for the contribution of a wide range of longitudinal velocities to gain in this scheme, considering that the total phase-space electron distribution is conserved by Liouville's theorem. The answer is that the electrons injected into the first wiggler must be within the angular range allowed by Eq. (42), which implies that the angle v_x/v_z must be well defined. This restriction is a substitute for the longitudinal velocity spread limits in usual FELs. It is nevertheless much less stringent than in our single quantum FEL-LWI scheme [3], where the collimation angle had to be of the order of the small recoil parameter (10^{-5} or less), so as to ensure distinguishability between electron momentum states after emission or absorption of only one photon.